Propagation and termination steps in Rh-mediated carbene polymerisation using diazomethane

Franssen, N.M.G.; Finger, M.; Reek, J.N.H.; de Bruin, B.

DOI
10.1039/c2dt32584e

Publication date
2013

Document Version
Final published version

Published in
Dalton Transactions

Dalton Transactions

RSC Publishing

PAPER

View Article Online
View Journal | View Issue

Cite this: *Dalton Trans.*, 2013, **42**, 4139

Propagation and termination steps in Rh-mediated carbene polymerisation using diazomethane†

Nicole M. G. Franssen,[a,b] Markus Finger,[a,b] Joost N. H. Reek[a] and Bas de Bruin*[a]

Rh-mediated carbene (co)polymerisation of diazomethane works best in the presence of Rh^{III} catalyst precursors, the use of which leads to a significant increase in polymer yield and molecular weight. Chain termination *via* β-hydride elimination is severely suppressed for these species, although this process does still occur leading to unsaturated chain ends. Subsequent chain walking leading to the formation of branched polymers seems not to occur. Computational studies describing pathways for both chain propagation and chain termination using a (cycloocta-2,5-dien-1-yl)Rh^{III}(alkyl) species as a representative model for the active species revealed that chain propagation is favoured for these species, although β-hydride elimination is still viable at the applied reaction temperatures. The computational studies are in excellent agreement with all experimental results, and further reveal that chain propagation *via* carbene insertion (leading to linear poly-methylene) occurs with a much lower energy barrier than insertion of 1-alkenes into either the Rh–H bond after β-hydride elimination or into the Rh–C bond of the growing polymer chain (leading to branched polymers). These energetic differences conveniently explain why experimentally the formation of branches is not observed in (co)polymerisation reactions employing diazomethane. The formation of substantial amounts of low-M_w oligomers and dimers in the experimental reactions can be ascribed to the presence of (1,5-cyclooctadiene)Rh^{I} species in the reaction mixture, for which chain termination *via* β-hydride elimination is clearly favoured over chain propagation. These two species stem from a non-selective catalyst activation process during which the catalyst precursors are *in situ* activated towards carbene polymerisation, and as such the results in this paper might contribute to further improvements of this reaction.

Received 29th October 2012,
Accepted 5th December 2012

DOI: 10.1039/c2dt32584e

www.rsc.org/dalton

Introduction

Polymers bearing polar functionalities are highly desired materials, since they exhibit beneficial properties with respect to adhesion and surface chemistry.[1] Despite recent advances in the field, it still remains a challenge to synthesise these materials in a controlled manner. The ideal would be to develop a process that yields high molecular-weight polymers with tunable amounts of polar functionalities and allows sequential insertions of polar monomers in a stereoselective manner.

In a previous publication[2] we have shown that we could obtain such functional polymers with tunable amounts of functional groups *via* carbene polymerisation (for reviews of this topic see ref. 3–5). In that paper we described a Rh catalysed copolymerisation reaction of diazomethane (DM) and ethyl diazoacetate (EDA) (Scheme 1). The best polymerisation results were obtained in the presence of Rh^{I} complex **1** (Scheme 1) and the amount of functionalities can be easily tuned by changing the monomer ratio or the way of addition.[2]

This copolymerisation approach works best when excess EDA is present in the reaction mixture (with respect to DM),

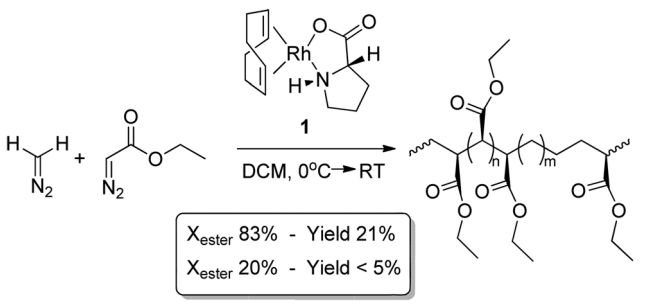

Scheme 1 Rh catalysed carbene polymerisation of diazomethane and ethyl diazoacetate.

[a]*Van't Hoff Institute for Molecular Sciences (HIMS), Department of Homogeneous and Supramolecular Catalysis, Universiteit van Amsterdam, P.O. Box 94720, 1090 GS Amsterdam, The Netherlands. E-mail: b.debruin@uva.nl; Fax: +31 20 525 5604; Tel: +31 20 525 6495*

[b]*Dutch Polymer Institute DPI, P.O. Box 902, 5600 AX Eindhoven, The Netherlands*

†Electronic supplementary information (ESI) available: The *x*, *y*, *z* coordinates and pdb files of the calculated structures. See DOI: 10.1039/c2dt32584e

and the resulting copolymers with high ester content (*i.e.*, above 50%) are obtained in good yields. Upon increasing the DM : EDA ratio, the incorporation of DM into the copolymers increases correspondingly, but the polymer yield and molecular weight drop significantly. This feature was ascribed to the occurrence of rapid β-hydride elimination after multiple consecutive insertions of DM, leading to the formation of short polymers/oligomers.

This rapid β-hydride elimination was confirmed by studying the homopolymerisation of DM, during which mainly ethene (*i.e.*, the dimer) and low molecular-weight (M_w) oligomers bearing unsaturated chain ends were formed. Only a small fraction of the DM was converted to higher M_w polymers which, despite rapid chain termination *via* β-hydride elimination, proved to be linear. Similar results were obtained for the copolymers of DM and EDA, in which the presence of branches could not be detected. These results indicate that the behaviour of DM in the presence of Rh catalyst **1** is rather different from that of EDA, for which β-hydride elimination does not or hardly occurs.[6] A mechanistic study concerning the (co)polymerisation behaviour of DM could contribute to a better understanding of the different behaviour of DM compared to EDA.

Previous mechanistic studies on the homopolymerisation of EDA revealed that the active species responsible for the propagation steps leading to the formation of high-M_w polymers is formed *in situ* from pre-catalyst **1**, likely involving reactions with EDA. This activation process is not selective towards the formation of one active species, but rather leads to the formation of several (at least four) active species with different structures and activities.[7] The diene ligand remains coordinated to the Rh centre during polymerisation, while the proline ligand leaves the coordination sphere after the initiation process.[5] Based on these data, a (cod)Rh^{I}(alkyl) species **2** was proposed as potentially active species involved in the formation of high-M_w copolymers (Fig. 1).[8] Recently, we found that, under the applied reaction conditions in the EDA homopolymerisation, activation of complex **1** leads as well to the formation of (cycloocta-2,5-dien-1-yl)-Rh^{III}(alkyl)$^{+}$ species **3** (Fig. 1).[9] This species contains an allyl-Rh^{III} fragment derived from (cod)Rh^{I}. Mechanistic studies suggest that species similar to **3** are most likely the active species in the homopolymerisation of EDA leading to the formation of high-M_w polymers.

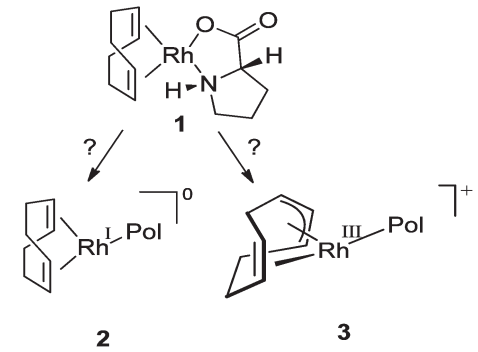

Fig. 1 Two likely candidates for the catalytically active species derived from precatalyst **1**.

Assuming that the catalyst activation process occurs in a similar manner in the presence of DM as for EDA (possible catalyst activation steps are depicted in Scheme 2), we can expect that both (cod)Rh^{I}(alkyl) species **2** and the Rh^{III} species **3** are present in the reaction mixture during DM polymerisation and could potentially contribute to the reaction (carbene dimerisation, oligomerisation or polymerisation). Since DM is much more reactive than EDA[2] and clearly reveals different chain-termination behaviour, its behaviour towards Rh species **2** and **3** might well differ from that of EDA. In other words, it is not at all trivial that Rh^{III} species **3** is responsible for the

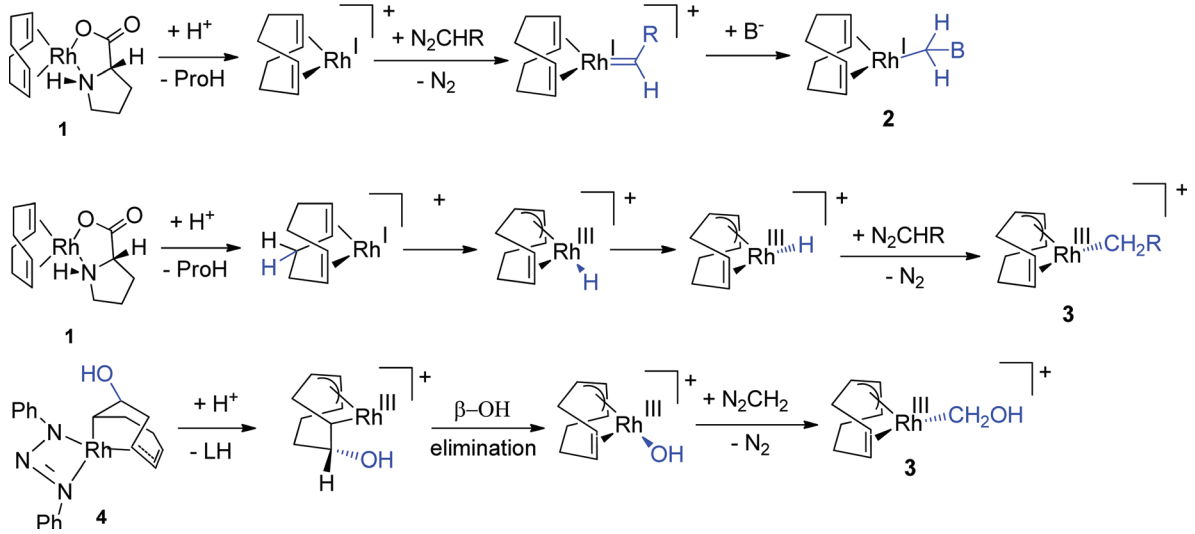

Scheme 2 Schematic representation of possible steps occurring during the activation of complex **1** to **2** (top), **1** to **3** (middle) and **4** to **3** (bottom) under the applied reaction conditions.

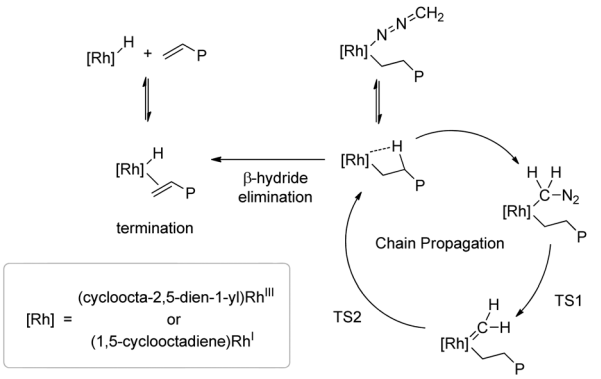

Scheme 3 Representation of the computationally-studied chain propagation and chain termination pathways for the reaction of DM in the presence of a rhodium catalyst.

formation of (long) polymers from DM. In this case, Rh^{I} species **2** could well contribute, since the balance for chain propagation *versus* chain termination might well have shifted for DM compared to EDA.

In order to get some information about the possible roles of Rh^{III} species **3** in the (co)polymerisation of DM catalysed by species **1**, we experimentally studied the reaction of DM and EDA in the presence of a well-defined Rh^{III} catalyst. In this paper, the results of these experiments will be compared with those reported in our previous publication[2] and will be supported by a computational study concerning chain propagation and chain termination pathways for both the Rh^{III} and the Rh^{I} species (Scheme 3). With these studies we hoped to gain a deeper understanding of the 'real' active species responsible for the formation of high-M_w polymers from DM. We further aimed at finding an explanation for the observed absence of branches in the (co)polymers from DM. The combined information derived from this study should contribute to the development of more selective catalysts for the formation of high-M_w polymers from DM and may serve as a guideline to design improved conditions for the DM–EDA copolymerisation reactions.

Results and discussion

1. The behaviour of Rh^{III} in DM–EDA copolymerisation experiments

Inspired by the likely involvement of (cycloocta-2,5-dien-1-yl)-Rh^{III}(alkyl)$^{+}$ species **3** for obtaining high-M_w material in the homopolymerisation of EDA, we anticipated that the direct use of (a close analogue of) these (cycloocta-2,5-dien-1-yl)-Rh^{III}(alkyl) species as catalysts in the copolymerisation reaction of DM and EDA might also lead to improved results in terms of copolymer yield and M_w for these reactions. Thus far, selective formation of species **3** from precatalyst **1** (see Fig. 1) cannot be achieved, but mechanistic studies concerning the homopolymerisation of EDA revealed that species **3** is more readily and more selectively accessible starting from (cycloocta-2,5-dien-1-yl)Rh^{III}(triazenyl) species **4** (Fig. 2; for possible catalyst activation steps see Scheme 2).[4] If (cycloocta-2,5-dien-1-yl)-Rh^{III}(alkyl) species are also responsible for the formation of high-M_w polymers from DM, applying species **4** in the copolymerisation reaction of DM and EDA is expected to lead to at least somewhat improved results as compared to the results obtained with the Rh^{I} catalyst precursors reported in our previous paper.[2]

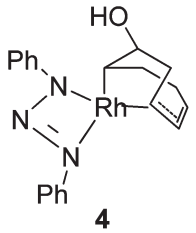

Fig. 2 (Cycloocta-2,5-dien-1-yl)Rh^{III}(triazenyl) species **4**.

Kinetic studies concerning the homopolymerisation of EDA with species **4** revealed that full conversion is achieved within 30 seconds, leading to the formation of mainly polymers. Addition of a second amount of monomer after the first 30 seconds allows continuation of the polymerisation and these monomers are added to the growing polymer chains.[9] Keeping in mind that we observed that polymerisation of DM occurs much faster than polymerisation of EDA under similar reaction conditions,[2] applying this approach to the copolymerisation of DM and EDA could theoretically facilitate the formation of high-M_w blocky copolymers from DM and EDA in which the block length of the DM block is determined by the relative DM concentration.

With the above expectations in mind, we set out to study the behaviour of species **4** in the copolymerisation of DM and EDA. We supplied a mixture of DM and EDA in a 1 : 1 ratio to a solution of **4** in dichloromethane. After 30 seconds, a second batch of the DM–EDA mixture was added to the catalyst, followed by a third batch after 4 hours of reaction time. Under these conditions, the copolymers were obtained in 10% yield (*vide infra*) and showed a M_w of 10 kDa based on NMR (Fig. 3; see our previous paper[2] for more detailed information about copolymer characterisation). The amount of DM in this copolymer sample is 96%, and the ester groups are present as $(CH(COOEt))_n$ blocks as well as randomly placed (*i.e.*, CH_2–CH-(COOEt)–CH_2). End groups were observed as CH_3 units (obtained by protonation similar to EDA homopolymers[7]) as well as unsaturated units ($CH{=}CH_2$ and $CH{=}CH$) pointing towards chain termination *via* β-hydride elimination. The low ester content in these copolymers indicates that most of the chain termination occurred before all DM was converted, thereby prohibiting the less reactive EDA monomers from being incorporated in large amounts into the growing polymer chain. As stated above, EDA was converted in 30 seconds in the homopolymerisation reaction. Since DM reacts faster than EDA, the low ester content also implies that chain termination most likely took place during the first moments of the

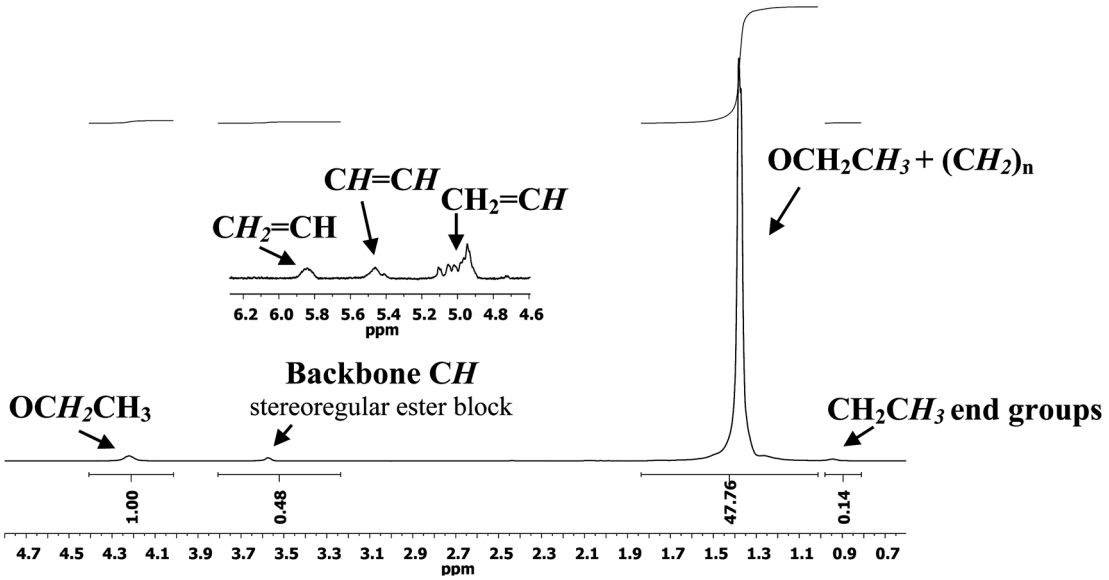

Fig. 3 ^{1}H NMR spectrum of the copolymers obtained in the DM–EDA copolymerisation catalysed by species **4** (1,2-dichlorobenzene-d_4, 80 °C).

reaction. The third mixture of DM and EDA added after 4 hours of reaction time is therefore no longer converted to polymers, since the active species for polymerisation had become inactive at that time due to chain termination (assuming that chain-transfer does not occur under these conditions[3]). This probably also holds for the addition of the second batch of EDA/DM after 30 seconds, but without detailed kinetic information about DM consumption under these conditions, incorporation of *some* of the DM added after 30 seconds into the growing polymer chain cannot be excluded. The above-listed yield for this copolymerisation reaction is based on the amount of monomers added in the first two batch additions.

Comparable results were obtained in the homopolymerisation reaction of DM in the presence of catalyst **4**. In this experiment we subjected the catalyst to a solution of DM in DCM and after 30 seconds we added the second batch of DM. This led to the formation of DM homopolymers with a M_w of *ca.* 10 kDa based on NMR in 18% yield. Hence, both the polymethylene yield and the polymer lengths obtained with catalyst **4** are substantially longer than those obtained with **1** (which produces mostly ethene, some $H_2{=}CH(CH_2)_nCH_3$ (n = 0–5) oligomer and <5% of solid polymer).

The above results show that species **4** indeed performs much better in the copolymerisation of DM and EDA when aiming for the synthesis of polymers with a high methylene (CH_2) content, both in terms of polymer yield and molecular weight compared to similar copolymers prepared with the Rh^I catalysts used in our previous publication.[2] The high methylene content in these copolymers shows that chain termination after several DM insertions (thereby leading to short oligomers) is severely suppressed for these species and thus indicates that the active species responsible for the formation of high-M_w polymers from DM is most likely also a Rh^{III} species derived from (cycloocta-2,5-dien-1-yl)Rh^{III}(alkyl)$^+$ species **3**. The improved activity of complex **4** in the homopolymerisation reaction of DM underlines that DM is most likely polymerised by a Rh^{III} species. However, chain termination *via* β-hydride elimination does still occur for this species, even for the high-M_w polymers. This does not only hamper the synthesis of copolymers with a blocky microstructure, but also indicates that formation of branched copolymers could in principle occur. As reported in our previous paper, the DM–EDA copolymers by Rh catalysis seem to be linear, which is rather surprising since most late transition-metal catalysts readily undergo chain walking after β-hydride elimination (*i.e.*, rotation of the alkene fragment and reinsertion) leading to branches. To get a better understanding of the behaviour of DM in the presence of these (cycloocta-2,5-dien-1-yl)Rh^{III}(alkyl) species, we performed a computational study in which we calculated the energy profile for both chain propagation and chain termination from species **3**.

2. DM polymerisation investigated computationally

2.1. Chain propagation at (allyl)Rh^{III}(alkyl) species. The smallest model structure that realistically represents the environment at active species **3** (in Et_2O) is the cationic dimethyl ether-solvated species [(allyl)Rh^{III}($(CH_2)_3$Me)(OMe_2)]$^+$ (**A**). This species can be considered to be formed by three consecutive methylene insertions (generated from DM) into a Rh–methyl bond (Fig. 8). We found that DM homopolymerisation yields somewhat higher amounts of polymer in the presence of diethyl ether as a solvent, and therefore the active species is best represented as the ether adduct (to minimise the complexity of the structure, dimethyl ether was taken as a smaller analogue of diethyl ether).

The lowest energy optimised geometry of **A** reveals a β-agostic interaction of the alkyl group with the metal. This

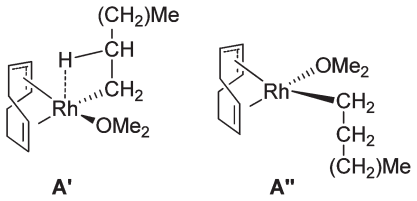

Fig. 4 Representation of higher-energy structures **A′** and **A″**.

complex adopts a distorted octahedral geometry, in which the polymer chain is located *trans* to the C=C fragment of the cycloocta-2,5-dien-1-yl ligand with the chain pointing in the direction of the (CH_2–CH_2) fragment of the allylic cycloocta-2,5-dien-1-yl ligand. The agostic interaction takes place in a *trans* fashion with respect to the allyl fragment of the cycloocta-2,5-dien-1-yl ligand. A similar structure is obtained for the complex in which the chain points in the direction of the $CHCH_2CH$ fragment of the cycloocta-2,5-dien-1-yl ligand (**A′**, Fig. 4), but this geometry has a slightly higher energy (+1.1 kcal mol^{-1}). The analogous complex in which the polymer chain is coordinated *trans* to the allyl moiety (**A″**, Fig. 4) has a substantially higher energy (+3.3 kcal mol^{-1}) than complex **A** (Fig. 8). Therefore this geometry (in which the species also shows no β-agostic interaction) was not considered further in the reaction profile with DM.

Binding of DM to (allyl)Rh^{III} species **A** *via* its carbon atom is exothermic, thus leading to the formation of complex **B** (−3.8 kcal mol^{-1}) in which the DM is positioned *trans* with respect to one of the terminal carbon atoms of the allyl moiety of the cycloocta-2,5-dien-1-yl ligand (*i.e.*, at the position of the agostic interaction in species **A**). In structure **B** the polymer chain has rotated around the Rh–C bond in the direction of the allyl fragment and is now pointing away from both the Rh centre and the allyl fragment (Fig. 5). In terms of free energy, coordination of DM to the Rh^{III} centre is slightly endergonic in the gas phase (+5.2 kcal mol^{-1}). However, gas-phase calculations overestimate translational entropy contributions for reactions in solutions. If we correct towards 'solution phase' entropy values (condensed phase reference volume and additional translational corrections in a Trouton-like approach), formation of **B** is roughly energy neutral (about −1 kcal mol^{-1}; for a complete overview of the related energies and corrections, see Table S1 in the ESI†).[10] Coordination of DM *via* its terminal N atom (species **B′**) is also exothermic (−8.4 kcal mol^{-1}). We were unable to find a plausible transition state that allows formation of a metal–carbene species directly from **B′**, which is in agreement with literature reports describing that formation of metal–carbene species from complexes analogous to **B′** takes place *via* an η^1-C intermediate similar to **B**.[11,12] Therefore this species **B′** was not taken into further consideration.

The loss of dinitrogen to form carbene species **C** seems to be the overall rate-determining step of the polymerisation reaction, similar to that observed for EDA polymerisation.[8] The enthalpic energy barrier for this process from **B** is +6.4 kcal

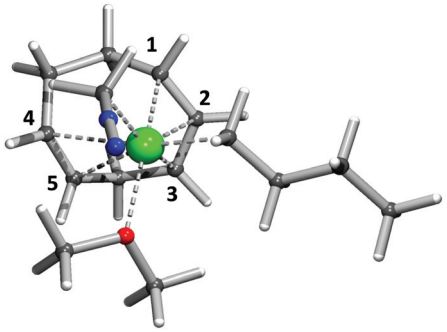

Fig. 5 DFT-optimised geometry of DM-adduct **B**, showing the orientation of the polymer chain (b3-lyp, def2-TZVP). Selected structural parameters: Rh–C1 2.123 Å; Rh–C2 2.137 Å; Rh–C3 2.302 Å; Rh–C4 2.624 Å; Rh–C5 2.547 Å; Rh–C_{diazo} 2.218 Å; Rh–C_{alkyl} 2.095 Å; C1–C2 1.433 Å; C2–C3 1.393 Å; C4–C5 1.348 Å; C_{diazo}–Rh–C_{alkyl} 86°.

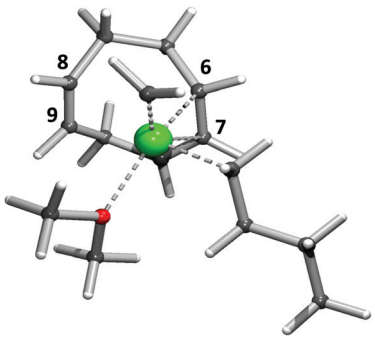

Fig. 6 DFT-optimised geometry of carbenoid **C**, showing the orientation of the carbene fragment and the detached double bond (lower left corner) (b3-lyp, def2-TZVP). Selected structural parameters: Rh–C6 2.093 Å; Rh–C7 2.367 Å; Rh–C8 2.676 Å; Rh–C9 2.704 Å; Rh–$C_{carbene}$ 1.834 Å; Rh–C_{alkyl} 2.087 Å; C6–C7 1.344 Å; C8–C9 1.463 Å; $C_{carbene}$–Rh–C_{alkyl} 86°.

mol^{-1} (**TS1** +2.6 kcal mol^{-1}) and the formation of species **C** is exothermic (−16.6 kcal mol^{-1}). In terms of free energy the activation barrier amounts to +11.9 kcal mol^{-1} in the gas phase, which translates to an activation barrier of about +6.7 kcal mol^{-1} in solution. Upon formation of the Rh–carbene species **C** from **B** the allyl moiety changes its coordination mode from η^3 (π-allyl) to η^1 (σ-allyl), and hence the allyl fragment occupies only one vacant site at the metal centre instead of two (Fig. 6). The olefinic C=C double bond of the cycloocta-2,5-dien-1-yl ligand is no longer coordinated to the metal in species **C**. The carbene points towards the (CH_2–CH_2) motif of the cycloocta-2,5-dien-1-yl ligand and the partly-detached allyl fragment allows optimal π-backbonding to the carbene fragment. The orientation of the carbene is perpendicular to the olefinic C=C fragment of the cycloocta-2,5-dien-1-yl ligand but parallel to the horizontal mirror plane through the polymer chain. As such the carbene moiety must rotate before it is able to undergo migratory insertion into the Rh–C bond. Despite this, migratory insertion of the carbene fragment into the Rh–C bond to form the insertion product **D′** occurs almost without a barrier (**TS2** +0.9 kcal mol^{-1} w.r.t. **C** (Fig. 7)).

The insertion process is calculated to be highly exothermic (**D′** −57.5 kcal mol^{-1}) (Fig. 8). In the transition-state structure **TS2**, rotation of the carbene moiety allows the allyl moiety of the cycloocta-2,5-dien-1-yl ligand to return to an η^3 coordination mode (π-allyl), as these moieties no longer compete for the same Rh d-orbital for π back-donation. At the same time, the coordination of the olefinic C=C double bond of the cycloocta-2,5-dien-1-yl ligand to the metal centre is restored.

After insertion of the carbene fragment the polymer chain formally ends up *trans* to the allyl moiety of the cycloocta-2,5-dien-1-yl ligand, but since this conformation is rather high in energy the complex adopts a distorted conformation **D′** in which the polymer chain has moved away from the *trans* influence of the allyl moiety to adopt a *cis*-like conformation. This structure rearranges easily to the more stable *cis*-conformation **D** (−58.9 kcal mol^{-1}), which is similar to that of **A.**

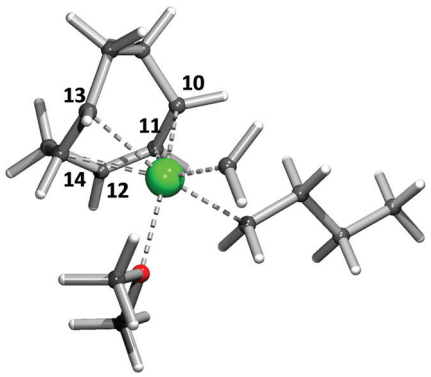

Fig. 7 DFT-optimised geometry of **TS2** (b3-lyp, def2-TZVP). Selected structural parameters: Rh–C10 2.078 Å; Rh–C11 1.854 Å; Rh–C12 2.640 Å; Rh–C13 2.391; Rh–C14 2.386 Å; Rh–$C_{carbene}$ 1.854; Rh–C_{alkyl} 2.229 Å; C10–C11 1.461 Å; C11–C12 1.365 Å; C13–C14 1.367 Å, $C_{carbene}$–C_{alkyl} 2.338 Å; $C_{carbene}$–Rh–C_{alkyl} 69°.

2.2. Chain termination from (allyl)Rh^{III}(alkyl) species. Since the above-described experiments suggest that β-hydride elimination followed by alkene dissociation is the main chain-termination pathway in DM polymerisation catalysed by species **3**, we next computationally investigated this pathway from species **A** (Fig. 9 and Table S2 in the ESI†).

β-Hydride elimination from **A** produces species **E**, in which the alkene fragment remains coordinated to the Rh centre. According to the computational results (Fig. 9 and Table S2 in the ESI†), formation of **E** is endothermic by +6.0 kcal mol^{-1}. Remarkably, the transition state for this process (Fig. 11) has a negative activation enthalpy for the back reaction. The fact that the transition state for β-hydride elimination is lower in enthalpy than **E** is a result of the vibrational thermal corrections. At the ZPE-corrected SCF level the transition state is well defined (−371 cm^{-1}), and somewhat higher in energy than **E** and **A** (see Table S2 in the ESI†). In any case, **TS3** is very close in (SCF) energy to **E.** Hence it is perhaps best to simply state that the back reaction of this endergonic process (*i.e.*, the reaction from **E** *via* **TS3** to **A**) is virtually barrierless. At the free-energy surface, a minor positive activation barrier is calculated

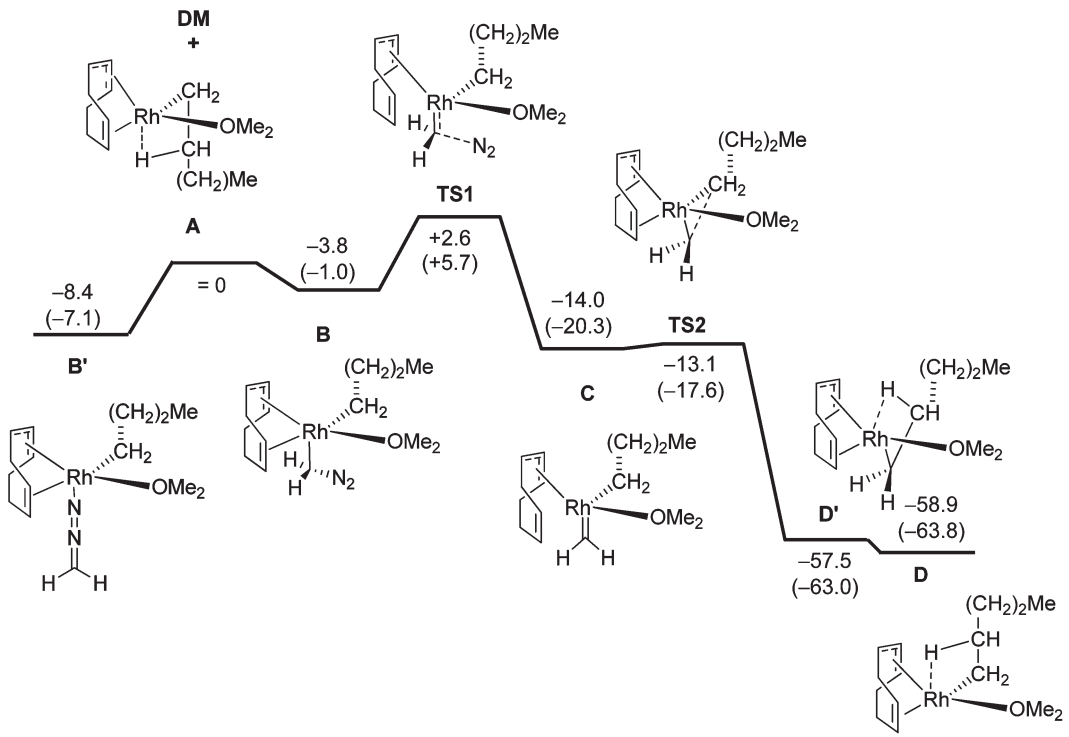

Fig. 8 General representation of the calculated chain propagation pathway (b3-lyp, def2-TZVP) from complex **A**, involving carbene formation and carbene insertion into the Rh–C bond of the growing chain. ΔH^0 values ($\Delta G_{solution}$ values between brackets) in kcal mol^{-1}.

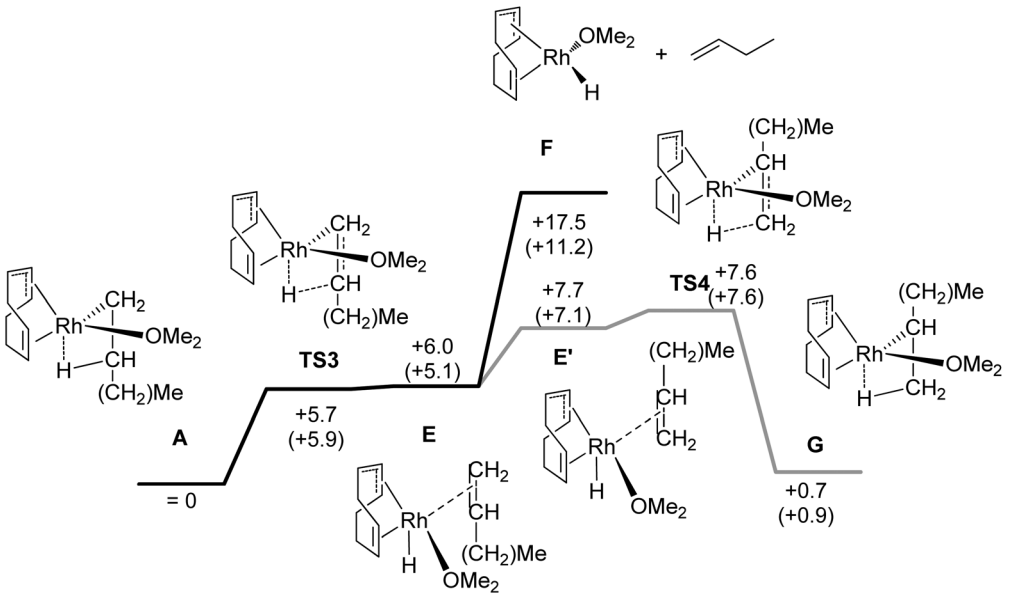

Fig. 9 General representation of the calculated chain-termination pathway from complex **A** (b3-lyp, def2-TZVP) involving β-hydride elimination followed by alkene dissociation. The gray lines represent insertion of the alkene fragment after rotation to initiate the pathway leading to branched polymers. ΔH^0 values ($\Delta G_{solution}$ values between brackets) in kcal mol^{-1}.

for the reaction from **E** to **A** ($\Delta G^{\ddagger}$ = +0.8 kcal mol^{-1}, see Table S2 in the ESI†).

Importantly, it is clear that the back reaction from **E** to **A** by reinsertion of the alkene into the Rh–H bond of species **E** occurs easily. At the same time, gaseous alkene dissociation from **E** is strongly endothermic (+11.5 kcal mol^{-1} with respect to **E**, +17.5 kcal mol^{-1} with respect to **A**) and endergonic with respect to **A** (+5.1 kcal mol^{-1}).[13] The overall free energy penalty for chain termination (β-hydride elimination followed by dissociation of *gaseous* alkenes) amounts to +5.9 kcal mol^{-1}. Keeping in mind that the binding energy of ethene to the Rh centre is underestimated[14] (in part due to the fact that in these calculations attractive van der Waals interactions are underestimated), the overall energy penalty for chain termination *via* β-hydride elimination will thus be substantially higher than +5.1 kcal mol^{-1}.

The termination of longer, *non-gaseous* (solvated) olefin chains requires an even higher energy penalty of at least +11.2 kcal mol^{-1} due to less favourable entropy contributions. This value is around 4.5 kcal mol^{-1} higher than the activation barrier for chain propagation *via* carbene insertion (+6.7 kcal mol^{-1}). At higher olefin concentrations (please keep in mind that the experimental catalytic species similar to species **3** present in the reaction mixture produce also substantial amounts of oligomers in the DM (co)polymerisation reactions (see section 1)), the driving force for the back reaction (*i.e.*, olefin reinsertion into the Rh–H bond) will be further enhanced compared to standard conditions. Thus, although the barrier for the actual β-hydride elimination process is perhaps within a reasonable range to proceed at the reaction temperature, this will not automatically lead to polymer termination. Furthermore, the energy penalty for chain termination from longer growing polymer chains in solution is much higher than the barrier for chain propagation.

This means that formation of relatively high-M_w polymers from (cycloocta-2,5-dien-1-yl)Rh^{III}(alkyl) species such as **A** can be expected in reactions with DM. This is in agreement with the above-described experimental results, in which relatively high-M_w polymers are indeed observed. The observation of unsaturated chain ends is in agreement with the energy profile calculated for chain termination *via* β-hydride elimination followed by alkene dissociation, which is disfavoured but still feasible at the applied reaction temperature.

2.3. Formation of branches. As described above, this Rh-mediated carbene polymerisation of DM could in principle also lead to formation of alkane-branched polymers, which could be formed by rotating the alkene fragment in structure **E** over 180° (leading to **E′**) followed by reinsertion of the alkene fragment into the Rh–H bond (*i.e.*, by a 2,1 insertion of the alkene fragment instead of a 1,2 insertion as is the case for the back reaction from **E**) (see Fig. 9 and Table S2 in the ESI†). Complex **E′** is 1.7 kcal mol^{-1} higher in energy than **E** and subsequent reinsertion of the rotated alkene fragment into the Rh–H bond of **E′** to form complex **G** is almost barrierless (+0.5 kcal mol^{-1} with respect to **E′**), indicating that this process is viable at this temperature.

Species **G** could in principle participate in a propagation cycle, similar to species **A**, which leads to branches in the polymer chain. Such branches were not observed in the experimental polymerisation reactions (see our previous publication[2]), and hence we considered it important to investigate the possibility of chain propagation from species **G** computationally (see Fig. 10 and Table S3 in the ESI†). Binding of DM *via* its carbon atom to species **G** to yield species **H** is slightly

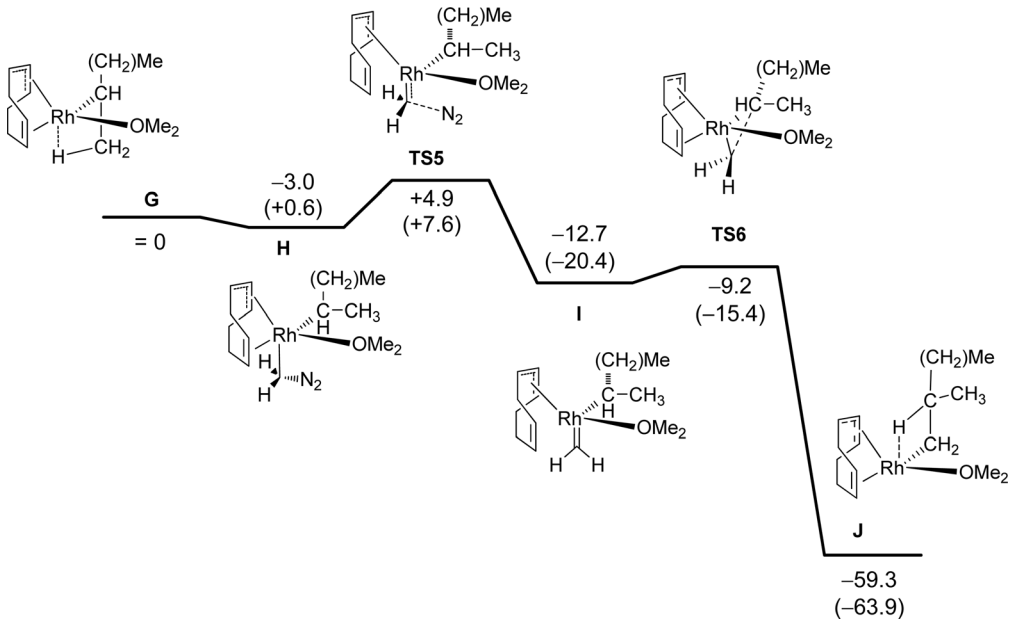

Fig. 10 General representation of the calculated chain propagation pathway (b3-lyp, def2-TZVP) from complex **G** leading to branched polymers, involving carbene formation and carbene insertion into the Rh–C bond of the growing chain. ΔH^0 values ($\Delta G_{solution}$ values between brackets) in kcal mol^{-1}.

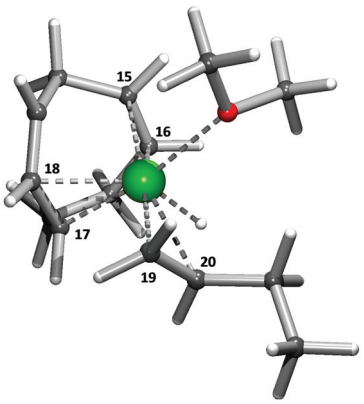

Fig. 11 DFT-optimised geometry of **TS3** (b3-lyp, def2-TZVP). Characteristic structural parameters: Rh–C15 2.366 Å; Rh–C16 2.330; Rh–C17 2.255 Å; Rh–C18 2.087 Å; Rh–C19 2.161 Å; Rh–C20 2.324 Å; Rh–H 1.579 Å; C20–H 1.759 Å.

exothermic (**H** −3.0 kcal mol^{-1}). Similar to species **B**, in this species **H** the DM is coordinated *trans* to the allyl moiety of the cycloocta-2,5-dien-1-yl ligand. Loss of dinitrogen is the rate-limiting step in this process (**TS5** +7.9 kcal mol^{-1}) and subsequent formation of carbenoid species **I** is exothermic (**I** −12.7 kcal mol^{-1}). Insertion of the carbene fragment into the growing polymer chain followed by rearrangement to the most stable conformation yields species **I** in a highly exothermic process and occurs with an enthalpy barrier of 3.5 kcal mol^{-1} (for the structure of **TS6**, see Fig. 13). This energy barrier is higher than the barrier observed for insertion of the carbene fragment into the linear polymer chain of species **C**, which is most likely a result of steric hindrance of the branch (*i.e.*, the additional CH_3 fragment) at the α-carbon of the growing chain. The total free-energy activation barrier for chain growth from a branched polymer fragment in 'solution' (**TS5**) is 7.9 kcal mol^{-1}, which is 1.5 kcal mol^{-1} higher than the activation barrier for extension of a linear polymer chain (**TS1**, Fig. 8 and Table S1 in the ESI†). As a result of this difference in energy barriers for propagation from **A** and **G**, the forward rate constant for propagation from **A** (or **D**) is 16 times larger than that for propagation from **G**. Formation of linear **D** from **A** is both kinetically and thermodynamically favoured over formation of chain-branched species **G** from **A**. Due to the energy difference between species **G** and species **A**, the concentration of species **A** in the reaction mixture is ~5.4 times higher than that of **G**. This, together with the larger rate constant for propagation from species **A**, leads to an ~86 times higher reaction rate for linear propagation compared to propagation from a branch. Combined with a higher barrier for formation of **G** from **A** than propagation from **A** to **D** ($\Delta\Delta G^{\ddagger}$ = +1.9 kcal mol^{-1}), the linear : branch ratio can be predicted to be even higher than 86 : 1. Since branched **G** should readily revert to linear **A** (*i.e.*, β-hydride elimination followed by reinsertion, see Fig. 9; Table S2 in the ESI†) and most of the (co)polymers of DM described in our previous paper contain only rather short blocks of DM (*i.e.*, less than 86 methylene units per block), these data readily explain why alkyl branches are not observed in the experimental carbene polymerisation reactions. The longer DM copolymers described in section 1 potentially contain longer DM blocks. Based on ^{1}H NMR integration, these blocks contain max. 5 branches per 1000 units. This correlates well with the above computational studies.

Formation of branches could in principle also occur by insertion of an alkene fragment (produced by olefin release after β-hydride elimination) into the Rh–C bond of an active

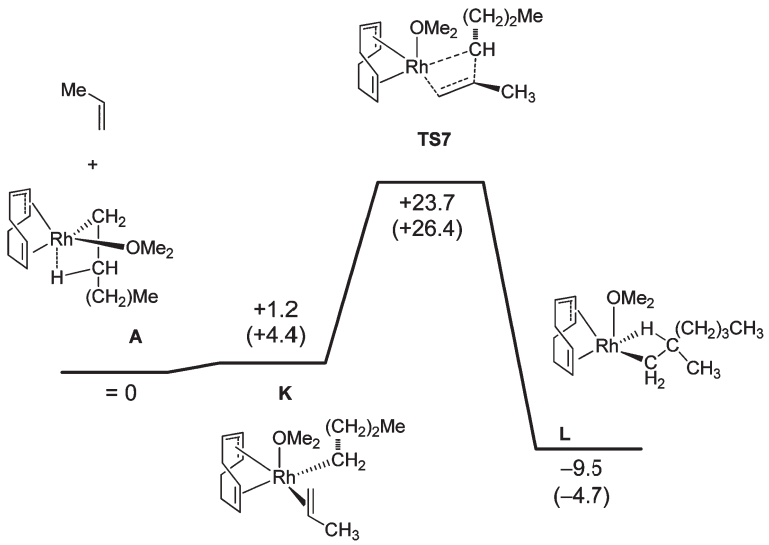

Fig. 12 General representation of the calculated chain propagation pathway (b3-lyp, def2-TZVP) from complex **A** leading to branched polymers, involving propene insertion into the Rh–C bond of the growing chain. ΔH^0 values ($\Delta G_{solution}$ values between brackets) in kcal mol^{-1}.

growing-chain Rh species (*i.e.*, species **A**). This would decrease the steric bulk around the metal centre, since in this case the branch is present at the β-carbon atom of the growing polymer chain, and as such lower barriers for subsequent chain propagation *via* DM insertion are expected. To study whether this pathway, potentially leading to branches, is viable at the applied reaction temperatures, we studied this possibility computationally for the (allyl)Rh^{III}(alkyl) species. We studied the insertion of propene as a representative model system for the insertion of 1-alkenes as a potential pathway to form alkyl-branched polymers (Fig. 12 and Table S4 in the ESI†). Coordination of propene to species **A** is slightly endothermic and leads to the formation of species **K** (+1.2 kcal mol^{-1}). In this species propene is coordinated *trans* to the allyl moiety of the cycloocta-2,5-dien-1-yl ligand similar to coordination of DM. The CH_3 group of the propene moiety is located at the side of the CH_2–CH_2 moiety of the cycloocta-2,5-dien-1-yl ligand but is pointing away from that ligand (Fig. 14). Coordination modes in which the methyl fragment of the propene is pointing towards the CH_2 fragment of the cycloocta-2,5-dien-1-yl ligand have a similar energy (**K′** +0.01 kcal mol^{-1}; Fig. 15). Coordination of propene with the CH_3 fragment pointing towards the cycloocta-2,5-dien-1-yl ligand, facing either its CH_2 fragment or the CH_2–CH_2 fragment, is slightly higher in energy (**K″** and **K‴** +1.2 kcal mol^{-1}; Fig. 15). In these species **K″** and **K‴** the OMe_2 fragment has dissociated from the Rh centre, and apparently this dissociation does not lead to a large increase in energy. The transition state for 1,2-insertion of propene occurs with a barrier of +23.7 kcal mol^{-1} (on the SCF level) and this transition state is accompanied by dissociation of the OMe_2 moiety from the Rh centre (Fig. 16). Release of the OMe_2 fragment has most likely only a small contribution to the total energy barrier, in a similar fashion as observed for species **K** *vs.* **K″** and **K‴**. The insertion of propene and rapid rearrangement of the conformation lead to the exothermic formation of

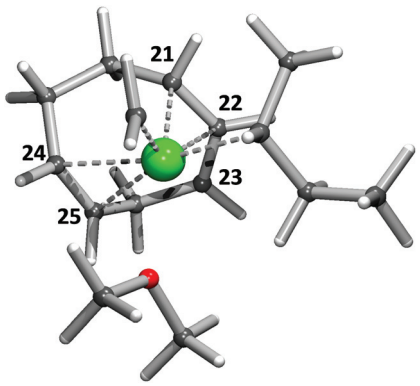

Fig. 13 DFT-optimised geometry of **TS6** (b3-lyp, def2-TZVP). Characteristic structural parameters: Rh–C21 2.073 Å; Rh–C22 2.318 Å; Rh–C23 2.689 Å; Rh–C24 2.410 Å; Rh–C25 2.419 Å; Rh–$C_{carbene}$ 1.845 Å; Rh–C_{alkyl} 2.275 Å; $C_{carbene}$–C_{alkyl} 2.390 Å; $C_{carbene}$–Rh–C_{alkyl} 70°.

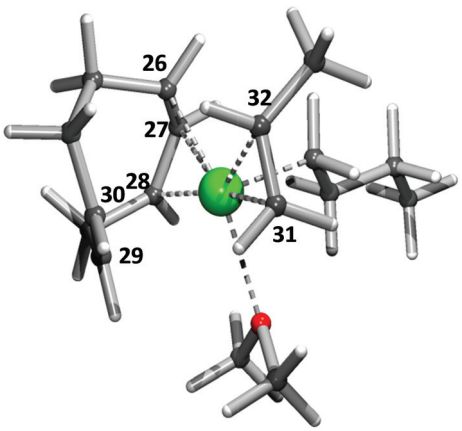

Fig. 14 DFT-optimised geometry of propene-adduct **K**, showing the orientation of the propene fragment with respect to the cycloocta-2,5-dien-1-yl ligand (b3-lyp, def2-TZVP). Characteristic structural parameters: Rh–C26 2.155 Å; Rh–C27 2.158 Å; Rh–C28 2.299 Å; Rh–C29 2.571 Å; Rh–C30 2.711 Å; Rh–C31 2.296 Å; Rh–C32 2.448 Å; Rh–C_{alkyl} 2.087 Å.

the insertion product **L** (−9.5 kcal mol^{-1}), in which the polymer chain is located *cis* with respect to the allyl moiety of the cycloocta-2,5-dien-1-yl ligand, similar to that described above for insertion of the carbene fragment (*cf.* species **D′** and **D**). The optimised geometry of this structure **L** reveals a β-agostic interaction between the β-hydrogen of the growing alkyl chain and the metal (Fig. 12), and coordination of the ether is restored. The energy barrier for propene insertion is much higher than that of DM insertion into the Rh–C bond of species **A**. Hence, chain propagation *via* DM insertion is largely favoured over 1-alkene insertion, disfavouring also 1-alkene insertion as a potential pathway leading to branching.

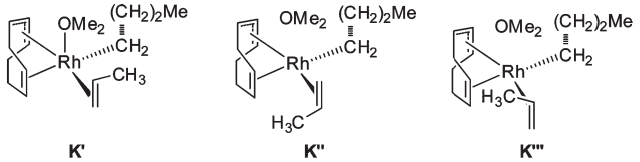

Fig. 15 Representation of propene-adducts **K′**, **K″** and **K‴**.

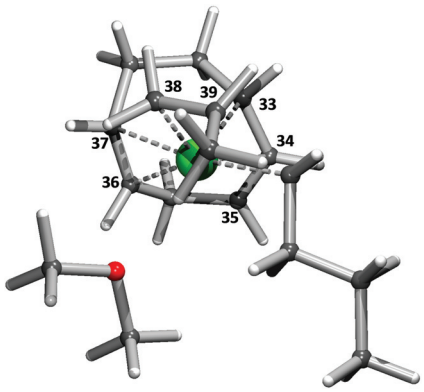

Fig. 16 DFT-optimised geometry of **TS7**, showing the rotated propene fragment and the dissociated OMe_2 fragment (b3-lyp, def2-TZVP). Characteristic structural parameters: Rh–C33 2.057 Å; Rh–C34 2.410 Å; Rh–C35 2.803 Å; Rh–C36 2.263 Å; Rh–C37 2.278 Å; Rh–C38 2.062 Å; Rh–C39 2.451 Å; Rh–C_{alkyl} 2.325 Å; Rh–O 3.015 Å; C39–C_{alkyl} 2.136 Å.

2.4 Oligomers and dimers: the role of (cod)Rh^{I}(alkyl) species. In the sections above we showed that (allyl)Rh^{III}(alkyl) species are responsible for the formation of high-M_w polymers from DM. However, the experiments described in section 1 and our previous publication yield large amounts of oligomers and dimers as undesired side products. Formation of these side products cannot be explained by the above-described reaction profiles for (allyl)Rh^{III}(alkyl) species, since for these species chain propagation is clearly favoured over chain termination. Therefore, we decided to study the involvement of (cod)Rh^{I}(alkyl) species also derived from species **1** (Fig. 1) as potential active species for the formation of these side products.

The smallest representative (cod)Rh^{I}(alkyl) model structure that realistically mimics the steric and electronic environment at the Rh^{I} polymerisation catalyst is (cod)Rh^{I}((CH$_2$)$_3$Me) species **M**, formed after three consecutive insertions of methylene units (generated from DM) into a Rh–methyl bond. The optimised geometry of this structure reveals a β-agostic interaction between the growing alkyl group and the metal (see Fig. 17). The corresponding δ-agostic complex is also feasible, although this structure has a somewhat higher energy (ΔG = +2.6 kcal mol^{-1}).

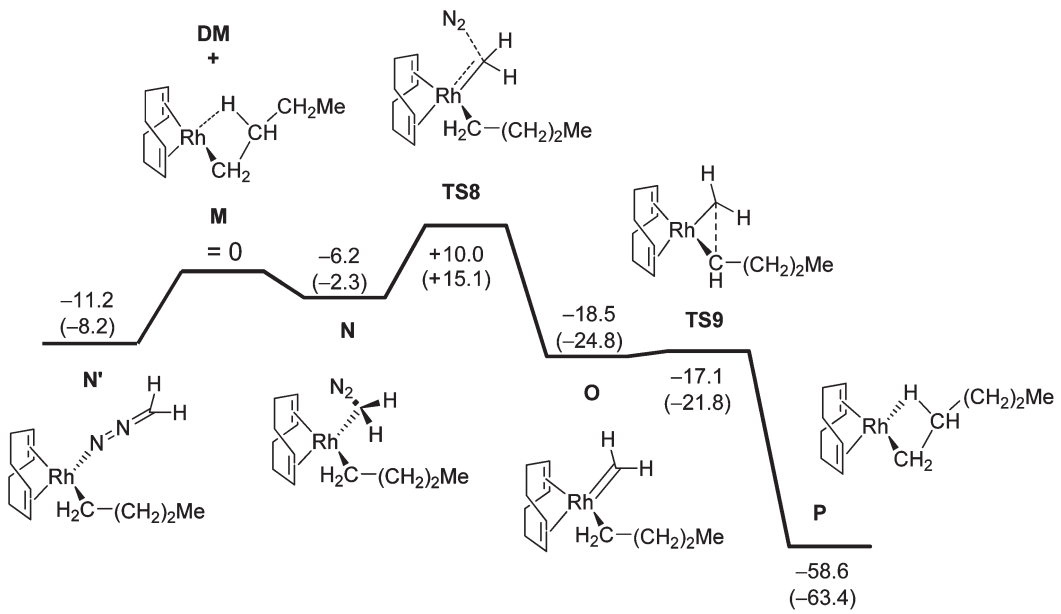

Fig. 17 General representation of the calculated chain propagation pathway (b3-lyp, def2-TZVP) from complex **M**, involving carbene formation and carbene insertion into the Rh–C bond of the growing chain. ΔH^0 values ($\Delta G_{solution}$ values between brackets) in kcal mol^{-1}.

Binding of DM to this structure *via* its central carbon atom leads to the formation of structure **N** (Fig. 17 and Table S5 in the ESI†), in which the β-agostic interaction is no longer observed. Binding of DM at **M** to form complex **N** is exothermic by 6.2 kcal mol^{-1}. DM coordination through its terminal nitrogen atom is also favourable (**N′**: ΔH^0 = −11.2 kcal mol^{-1}) but non-productive. We were unable to find a plausible transition state that allows formation of a metal–carbene species directly from **N′** and therefore this species was not taken into further consideration.

Formation of carbenoid species **O** from the carbon-bound DM adduct **N** proceeds readily *via* dinitrogen loss in transition-state **TS8**. This is the overall rate-limiting step along the calculated reaction pathway (Fig. 17). In both **O** and **TS8**, the (partial) Rh=C double bond adopts a parallel orientation with respect to the C=C double bond of the cod ligand *trans* to it (Fig. 18). In this way, the carbene fragment is pre-organised for subsequent migratory insertion into the Rh–C bond of the growing polymer chain.

Migratory insertion proceeds *via* a remarkably low-energy transition state (**TS9**, +1.4 kcal mol^{-1} w.r.t. **O**) to produce complex **P**. This reaction is calculated to be highly exothermic (**P** −58.6 kcal mol^{-1}). In the most stable conformation of **P** the β-agostic interaction between the growing chain and the metal is restored (similar to the interaction observed for structure **M**, which is logical since **M** is basically a one backbone-carbon shortened version of **P**).

We next computationally investigated chain termination from species **M**, involving β-hydride elimination followed by alkene dissociation (Fig. 19 and Table S6 in the ESI†).

Formation of (cod)Rh^{I}H(alkene) complex **Q** (Fig. 20) from complex **M** *via* β-hydride elimination is remarkably easy (**TS10**

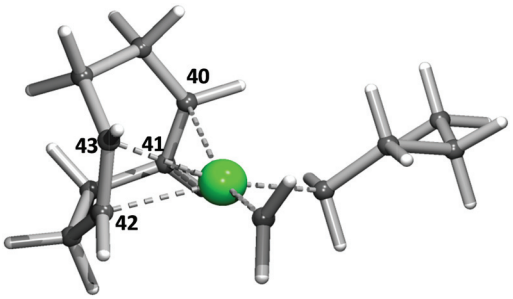

Fig. 18 DFT-optimised geometry of carbenoid **O**, showing the orientation of the carbene fragment (b3-lyp, def2-TZVP). Characteristic structural parameters: Rh–C40 2.394 Å; Rh–C41 2.457 Å; Rh–C42 2.271 Å; Rh–C43 2.226 Å; Rh–$C_{carbene}$ 1.813 Å; Rh–C_{alkyl} 2.143 Å; $C_{carbene}$–Rh–C_{alkyl} 94°.

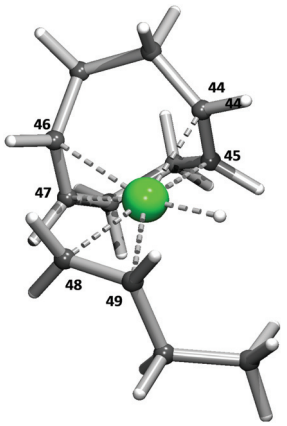

Fig. 20 DFT-optimised geometry of **Q** (b3-lyp, def2-TZVP). Characteristic structural parameters: Rh–C44 2.172 Å; Rh–C45 2.200 Å; Rh–C46 2.321 Å; Rh–C47 2.284 Å; Rh–C48 2.200 Å; Rh–C49 2.278 Å; Rh–H 1.579 Å.

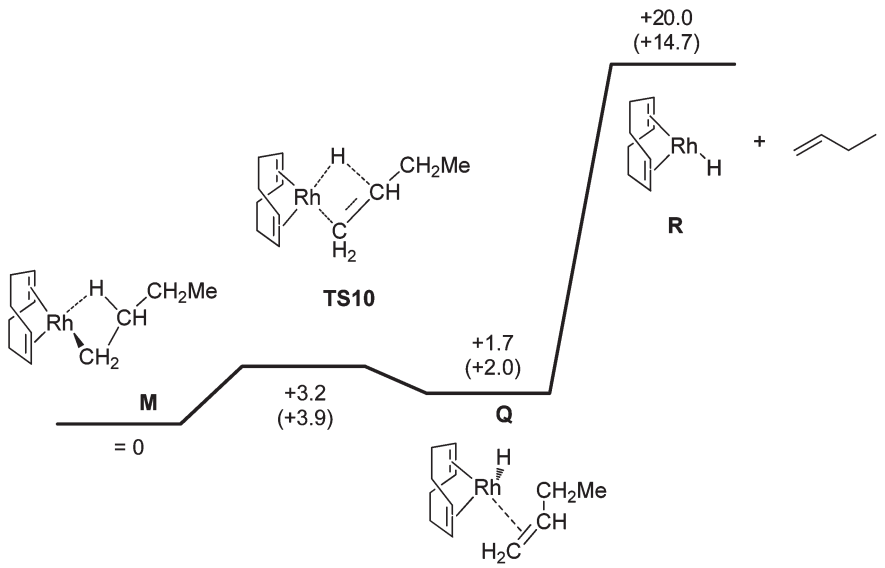

Fig. 19 General representation of the calculated chain-termination pathway from complex **M** (b3-lyp, def2-TZVP) involving β-hydride elimination followed by alkene dissociation. ΔH^0 values ($\Delta G_{solution}$ values between brackets) in kcal mol^{-1}.

+3.2 kcal mol^{-1}) and only marginally endothermic (+1.7 kcal mol^{-1}). However, release of the alkene and formation of (cod)-Rh^{I}-hydride species **R** are highly endothermic (+20.0 kcal mol^{-1}). In **R** the Rh centre adopts a distorted square planar geometry, in which the Rh–C distances of the double bond of the cod ligand coordinated *trans* to the hydride are elongated (the distance to the centre of the double bond is 2.2 Å *vs.* 2.0 Å). If the entropy contribution is taken into account, the release of gaseous alkenes from structure **Q** is not very endergonic (ΔG_{273K} = +8.5 kcal mol^{-1}), indicating that this process is viable at the applied reaction temperature. Release of non-gaseous (solvated) alkenes in solution is more endergonic (see Fig. 19) but the free energy for alkene loss is always lower than the free-energy barrier for chain propagation (see Table S6 in the ESI†).

The energy barrier for β-hydride elimination from species **M** is much lower than that for propagation by carbene insertion at the same species **M**. This low barrier for β-hydride elimination is in part counterbalanced by the endothermic release of the alkene fragment, but if entropy factors are included the overall process is still clearly in favour of β-hydride elimination followed by olefin dissociation (chain termination), especially in the case of gaseous olefins such as ethene, propene and butene. Elimination of higher (liquid/solvated) alkenes is also calculated to be favoured over chain propagation. Hence, according to the above computational data, the Rh^{I}(cod) species **M** should behave as a carbene dimerisation catalyst producing mainly ethene (at best an oligomerisation catalyst producing besides ethene also some propene, butene and pentene) in its reactivity towards DM as the carbene precursor. As such, the behaviour of this Rh^{I} species is clearly different from that of the above-discussed (allyl)Rh^{III}(alkyl) species and confirms its participation in oligomerisation/dimerization.

These computations clearly show that the experimental (co) polymerisation results using DM can be improved by diminishing the amount of (cod)Rh^{I} species in the reaction mixture. This should avoid the formation of undesired side products and subsequently increase the yield and M_w of the high-M_w polymers that are made by (allyl)Rh^{III}(alkyl) species. In order to achieve this, it is important to optimise the catalyst activation process in such a way that it selectively leads to the formation of (allyl)Rh^{III}(alkyl) species involved in polymerisation, and keeping the catalyst in this active form. The latter may not be trivial, as (re)formation of (1,5-cyclooctadiene)Rh^{I} complexes from (cycloocta-2,5-dien-1-yl)Rh^{III}(alkyl) species cannot at all be excluded,[15] and this may well explain the formation of low molecular weight side-products when starting from species **4** as a precatalyst. Research in our group is currently focussing on these open research questions.

Conclusions

Rh-mediated carbene copolymerisation of diazomethane and ethyl diazoacetate in the presence of (cycloocta-2,5-dien-1-yl)-Rh^{III} catalysts leads to improved results in terms of polymer yield and molecular weight as compared to our previously reported system using Rh^{I} catalyst precursors. For these (cycloocta-2,5-dien-1-yl)Rh^{III} species, chain termination *via* β-hydride elimination after several methylene insertions (derived from diazomethane) is severely suppressed, leading to copolymers containing 98% methylene units and 2% CHCOOEt units in 10% yield. These copolymers have a molecular weight of 10 kDa and chain ends were observed as –CH_3 and CH=CH_2 groups. This indicates that chain termination *via* β-hydride elimination does still occur although, surprisingly, subsequent chain walking leading to branches is strongly suppressed.

Computational studies describing the mechanistic steps for chain propagation and termination in the homopolymerization of diazomethane using (cycloocta-2,5-dien-1-yl)Rh^{III}(alkyl) species as a model for the catalytically active species revealed that chain propagation leading to high-M_w polymers is indeed favoured over chain termination *via* β-hydride elimination. These calculations reveal that β-hydride elimination occurs with a relatively low energy barrier and as such this process is, although disfavoured, still viable at the reaction temperature. This emphasises that these calculations are in good agreement with the new experimental results obtained with Rh^{III} catalysts.

According to these calculations, rotation of the alkene fragment after β-hydride elimination and reinsertion into the Rh–H bond occurs readily, but subsequent chain growth *via* carbene insertion from such α-branched intermediates leading to branched polymers occurs with a higher energy barrier than chain propagation from linear intermediates producing linear polymers. The significant energy differences between the activation barriers for carbene insertion from these intermediates explain the formation of (nearly) linear polymers in the (co)-polymerisation of diazomethane. Formation of branches *via* 1,2-insertion of 1-alkenes into the Rh–C bond of the growing polymer chain occurs with an even higher energy barrier than carbene insertion into that same bond, indicating that this pathway leading to the formation of branched polymers is also disfavoured with respect to carbene insertion polymerisation leading to linear high-M_w polymers.

The combined experimental and computational data point to formation of a mixture of (cycloocta-2,5-dien-1-yl)Rh^{III}(alkyl) and (1,5-cyclooctadiene)Rh^{I}(alkyl) species under the applied catalytic conditions. While the (cycloocta-2,5-dien-1-yl)-Rh^{III}(alkyl) species produce high-M_w polymers, the (1,5-cyclooctadiene)Rh^{I}(alkyl) species are responsible for formation of substantial amounts of low-M_w oligomers and dimers. Optimizing the catalyst activation process to minimise the amount of (1,5-cyclooctadiene)Rh^{I} species in the reaction mixture therefore seems to be a key factor to improve the (co)polymerisation results. For these species chain termination *via* β-hydride elimination is clearly favoured over chain propagation *via* carbene insertion, leading to (very) low-M_w side products. Whether or not (re)formation of (cod)Rh^{I} species is preventable is a current open research question.

Experimental section

DFT calculations

The geometry optimisations were carried out with the Turbomole program package[16] coupled to the PQS Baker optimiser[17] *via* the BOpt package.[18] Geometries were fully optimised as minima or transition states at the DFT/b3-lyp[19–22] level using the triple-ζ def2-TZVP basis set[23,24] (small-core pseudopotential at Rh[25,26]). All stationary points were characterised by vibrational analysis (analytical frequencies); ZPE and thermal corrections (enthalpy, 273 K, 1 bar) from these analyses are included. By calculation of the partition function of the molecules in the gas phase, the entropy of dissociation or coordination for reactions in solution is severely overestimated. For reactions in 'solution' we therefore corrected the Gibbs free energies for all molecules except N_2 by adding either 2.5 kcal mol^{-1} (correction purely for the condensed-phase reference volume, see ESI†)[27] or 6.2 kcal mol^{-1} (additional correction for the translational entropy in a Trouton-like fashion;[28,29] values between brackets in Fig. 8, 9, 10, 12, 17 and 19).

DM–EDA copolymerisation reactions

Complex **4** was prepared according to literature procedures.[21]

DM (*ca*. 1 mmol in 10 mL DCM) was prepared in a similar manner as described previously.[2] EDA (1 mmol) was added to this solution and the mixture was added to an ice-cooled solution of **3** (0.04 mmol) in DCM (2 mL). The reaction was stirred for 30 seconds at 0 °C, during which gas evolution took place. Subsequently, a fresh solution of DM (*ca*. 1 mmol) and EDA (1 mmol) in DCM (10 mL) was added to the reaction mixture and the reaction was stirred for 4 hours, during which it slowly warmed up to room temperature. At the end of these 4 hours the mixture was again cooled in an ice bath and a fresh solution of DM (1 mmol) and EDA (1 mmol) in DCM (10 mL) was added. After stirring for 16 hours, during which the temperature rose to room temperature, the mixture was concentrated *in vacuo* to *ca.* 4 mL and MeOH (20 mL) was added to precipitate the polymer. The suspension was centrifuged after which the supernatant was removed and the grey precipitate was allowed to dry *in vacuo*. Yield: 11 mg (0.34 mmol).

DM homopolymerisation reactions

The reactions were carried out in a similar fashion as described above for the copolymerisations of DM and EDA. Instead of adding a mixture of DM and EDA, we supplied a solution containing only DM (*ca*. 1 mmol) to catalyst **4** in DCM. Addition of a second batch of DM followed after 30 seconds, after which the reaction was allowed to warm to room temperature while the stirring was continued for 16 hours.

Acknowledgements

We thank the Dutch Polymer Institute DPI, PO Box 902, 5600 AX Eindhoven, The Netherlands (project #646 and #647), The University of Amsterdam (UvA) and the European Research Council (ERC, EU, 7th framework program, grant agreement 202886-CatCIR) for financial support.

Notes and references

1 A. Nakamura, S. Ito and K. Nozaki, *Chem. Rev.*, 2009, **109**, 5215.
2 N. M. G. Franssen, K. Remerie, T. Macko, J. N. H. Reek and B. de Bruin, *Macromolecules*, 2012, **45**, 3711.
3 E. Ihara, *Adv. Polym. Sci.*, 2010, **231**, 191.
4 E. Jellema, A. L. Jongerius, J. N. H. Reek and B. de Bruin, *Chem. Soc. Rev.*, 2010, **39**, 1706.
5 N. M. G. Franssen, A. J. C. Walters, J. N. H. Reek and B. de Bruin, *Catal. Sci. Technol.*, 2011, **1**, 153.
6 M. Finger, J. N. H. Reek and B. de Bruin, *Organometallics*, 2011, **30**, 1094.
7 A. J. C. Walters, E. Jellema, M. Finger, P. Aarnoutse, J. M. M. Smits, J. N. H. Reek and B. de Bruin, *ACS Catal.*, 2012, **2**, 2465; J.-Y. Dong and Y. Hu, *Coord. Chem. Rev.*, 2006, **250**, 47.
8 E. Jellema, P. H. M. Budzelaar, J. N. H. Reek and B. de Bruin, *J. Am. Chem. Soc.*, 2007, **129**, 11631.
9 A. J. C. Walters, O. Troeppner, I. Ivanović-Burmazović, C. Tejel, M. P. del Río, J. N. H. Reek and B. de Bruin, *Angew. Chem., Int. Ed.*, 2012, **51**, 5157.
10 One should keep in mind that the reported free energies in Tables S1–S6 in the ESI† are all standard values (*i.e.*, 1 bar partial pressures in the gas phase and 1 M concentrations of all species involved), while the polymerisation experiments are performed using an excess of DM with respect to the Rh catalyst. In previous papers concerning the homopolymerisation of EDA we reported that the initiation efficiency of the (cod)Rh(L-prolinate) precatalyst is rather low (~2%). Assuming that the initiation efficiency in the homopolymerisation of DM is of a similar order of magnitude, the excess DM used in the experiments with respect to the amount of *active* Rh^{III} species is even much larger than 50-fold. Under such non-standard conditions there is always a free-energy driving force for substrate binding ($\Delta G = \Delta G^0 + RT\ln Q$, in which Q is the reaction constant).
11 R. Cohen, B. Rybtchinski, M. Gandelman, H. Rozenberg, J. M. L. Martin and D. Milstein, *J. Am. Chem. Soc.*, 2003, **125**, 6532.
12 J. A. S. Howell, *Dalton Trans.*, 2007, 1104.
13 Ligand substitution at the 6-coordinate d^6 rhodium(III) complex **E** must follow a dissociative pathway.
14 S. Thewissen, *Reactivity in the Gas Phase and Solution of Group 9 Metal Olefin Complexes* (PhD thesis), 2005, Appendix A.

15 A likely pathway for (re)formation of (cod)Rh^{I} complexes from (cycloocta-2,5-dien-1-yl)Rh^{III}alkyl species involves β-hydride elimination from the alkyl and subsequent reductive elimination of the allyl and hydride moieties to form (cod)Rh^{I}.
16 R. Ahlrichs, *Turbomole Version 6.3.1*, Theoretical Chemistry Group, University of Karlsruhe.
17 *PQS version 2.4*, Parallel Quantum Solutions, Fayetteville, Arkansas (USA), 2001; the Baker optimiser is available separately from PQS upon request; I. Baker, *J. Comput. Chem.*, 1986, **7**, 385.
18 P. H. M. Budzelaar, *J. Comput. Chem.*, 2007, **28**, 2226.
19 C. Lee, W. Yang and R. G. Parr, *Phys. Rev. B: Condens. Matter*, 1988, **37**, 785.
20 A. D. Becke, *J. Chem. Phys.*, 1993, **98**, 1372.
21 A. D. Becke, *J. Chem. Phys.*, 1993, **98**, 5648.
22 Calculations were performed using the Turbomole functional 'b3-lyp', which is not completely identical to the Gaussian 'B3LYP' functional.
23 F. Weigend and R. Ahlrichs, *Phys. Chem. Chem. Phys.*, 2005, **7**, 3297.
24 F. Weigend, M. Häser, H. Patzelt and R. Ahlrichs, *Chem. Phys. Lett.*, 1998, **294**, 143.
25 Turbomole Basisset Library, *Turbomole Version 6.3.1*.
26 D. Andrae, U. Haeussermann, M. Dolg, H. Stoll and H. Preuss, *Theor. Chim. Acta*, 1990, **77**, 123.
27 W. I. Dzik, X. Xu, P. Zhang, J. N. H. Reek and B. de Bruin, *J. Am. Chem. Soc.*, 2010, **132**, 10891.
28 P. Deglman, E. Ember, P. Hofmann, S. Pitter and O. Walter, *Chem.–Eur. J.*, 2007, **13**, 2864.
29 N. Schneider, M. Finger, C. Haferkemper, S. Bellemin-Laponnaz, P. Hofman and L. Gade, *Angew. Chem., Int. Ed.*, 2009, **48**, 1609.

